Nanoscale

Life-time and line-width of individual quantum dots interfaced with graphene

Journal:	*Nanoscale*
Manuscript ID	NR-ART-03-2018-001769
Article Type:	Paper
Date Submitted by the Author:	01-Mar-2018
Complete List of Authors:	Miao, Xin; NJIT, ECE Gosztola, David; Argonne National Laboratory, Center for Nanoscale Materials Sumant, Anirudha; Argonne National Laboratory, Centre for NanoMaterials grebel, haim; NJIT, ECE

Lifetime and linewidth of individual quantum dots interfaced with graphene

Xin Miao[1], David J. Gosztola[2], Anirudha V. Sumant[2] and Haim Grebel[1,*]

[1]*Electronic Imaging Center and ECE Dept., New Jersey Institute of technology (NJIT), Newark, NJ 07102, USA.* grebel@njit.edu

[2]*Center for Nanoscale Materials, Nanoscience and Technology Division, Argonne National Laboratory Argonne, IL 60439*

Abstract: We report on luminescence lifetimes and linewidths from an array of individual Quantum Dots (QDs) that were either interfaced with graphene surface guides or dispersed on aluminum electrodes. The observed fluorescence quenching is consistent with screening by charge carriers. Fluorescence quenching is typically mentioned as a sign that chromophores are interfacing with a conductive surface (metal or graphene); we find that QDs interfaced with the metal film exhibit shortened lifetime and line-broadening but not necessarily fluorescence quenching as the latter may be impacted by molecular concentration, reflectivity and conductor imperfections. We also comment on angle-dependent lifetime measurements, which we postulate depend on the specifics of the local density-of-states involved.

I. Introduction:

Quenching of fluorescence in the vicinity of conductors is well documented [1-2]. There is growing interest in studying fluorescence quenching with graphene [3-5], a monolayer, or a few layers of graphite. Fluorescence quenching of quantum dots (QD) by graphene may be attributed

to an excitation in the QD followed by a physical transfer of electrons from the fluorophores to the graphene with applications to photodetectors in mind [6-14]. The energy transfer may also be induced through screening; an excited localized QD may interact with the collective charges in an adjacent conductor [15-18]. In this case, the resultant energy transfer between the QD and graphene is similar to FRET (fluorescence resonance energy transfer, which is enabled through screening by free-carriers in the graphene film. The process, which is also known as a Förster process, is enabled by the unique electronic dispersion of graphene [19]. These theories do not fully explain the fluorescence quenching in graphene because near the Dirac point such screening is linearly diminishing and the screening, if it exists, should be non-linear and dependent on the amount of charge placed within a small distance away from the graphene [20-21]. Thus, excited charge concentration within the QD and in the graphene, as well as the local conductivity of the conductor may be at issue. If fluorescence quenching is due to energy transfer between the chromophore and dipoles in the conductive film (metal or graphene), there will be an increase in the density-of-states for such a radiation outlet. Large density-of-states results in shorter lifetimes and broadening of the fluorescence line [22].

In light of concentration dependent signals [23], we set out instead to study isolated QDs. Screening by relatively thick QD films [24] and charge coupling between nearby dots may mask a local interaction with the conductor. In order to physically isolate the QDs from one another we placed individual QD in hole array formed in Anodized Aluminum Oxide (AAO) films. Such arrangement also lets us study coupling between the emission and surface graphene modes. The properties of graphene on periodic and porous substrates, such as AAO have been studied in conjunction with Surface Enhanced Raman (SERS) [25-26] and Surface Plasmon Polariton

(SPP) lasers [27-29]. In these substrates, the graphene is partially suspended over the substrate pores. For the energy transfer between the chromophore and graphene to be effective, the characteristic parameter $\alpha=e^2/(\varepsilon\hbar v_F)$ ought to be larger than 1 with ε, the dielectric constant of vacuum, e is the electron charge, $\hbar$ is the reduced Plank constant and v_F the Fermi velocity of the charge carriers [20]. Graphene over nanopores is attractive for several reasons: v_F is relatively small compared to a metal thus α is large; our structure places the excited charges a bit away from the graphene in a systematic way; the graphene is an excellent surface guide [29]. Study of quenching effects by graphene needs to take into account the absorption of graphene (~2.3% per layer) in comparison with the absorption of the CdSe/ZnS QD monolayer so that the film of dots does not screen itself [30]. We set to measure lifetimes and spectral linewidths of QDs interfaced with graphene and with an aluminum film. QDs embedded in a bare AAO hole-array were used as reference.

II. Experiments

A schematic of our substrate is shown in Fig. 1. Details of structure fabrication are provided in the Method section below. The aluminum electrode was part of the anodization process (Fig. 1c). The core/shell CdSe/ZnS QDs were coated with a ligand to prevent agglomeration while in suspension in the pore; the thickness of the ligand was ~8 nm and the diameter of the core/shell QD was ~10 nm [31] resulting in one dot per pore.

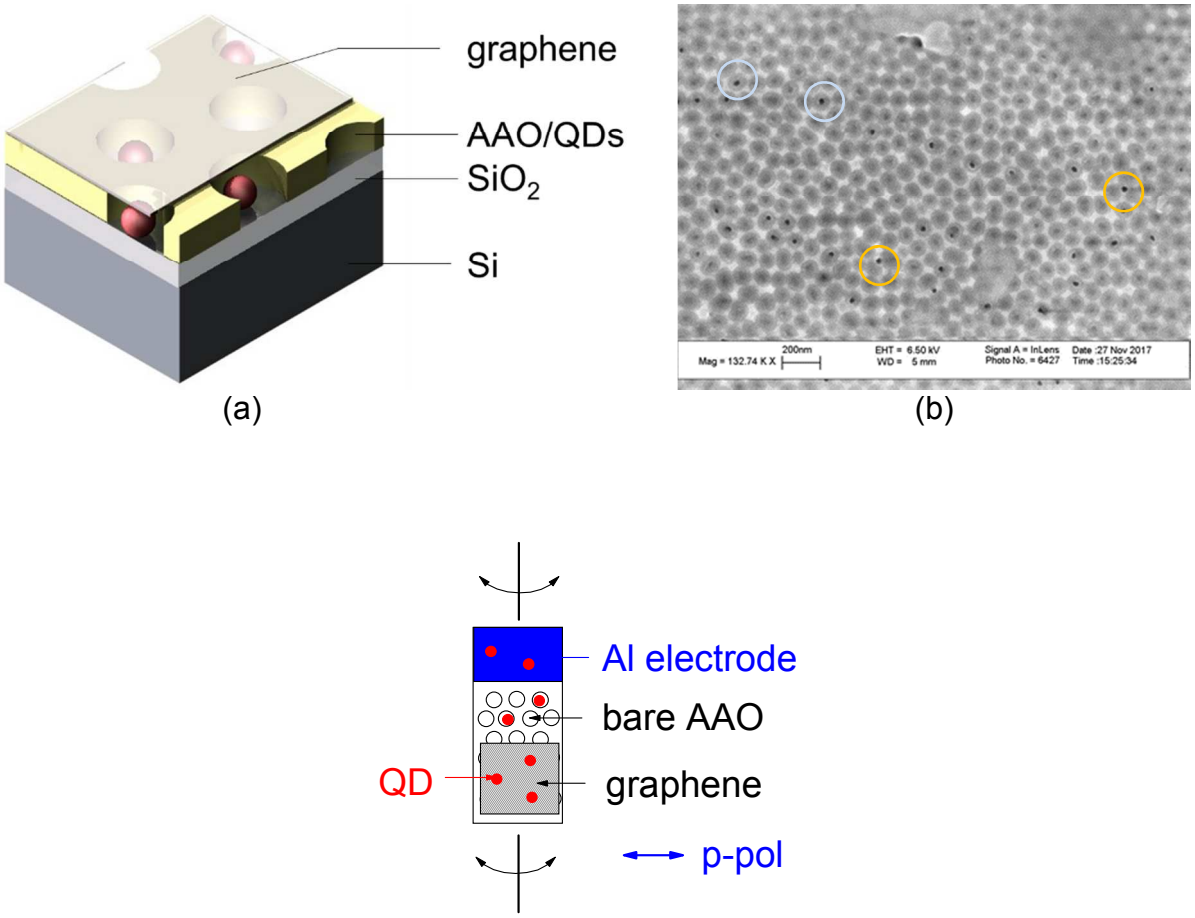

Fig. 1. (a) Schematics of graphene covered configuration. (b) SEM picture of QD-filled hole-array in anodized aluminum oxide (the black dots within the pores, some are marked by blue circles). Occasionally one may find QDs, marked by a yellow circle, between the holes. (c) Top view of the sample: the metal electrode, used for anodization, is situated right next to the AAO region. The graphene was covering part of the QD embedded AAO region. The sample was rotated as shown and the incident polarization was p-pol. with respect to sample axis.

III. Surface modes

The periodic structure in the AAO regions provides us with an effective way of coupling between surface and radiation modes. This coupling may affect the luminescence intensity as detected by a far-field detector and could impact the measured lifetime constants. Electromagnetic surface modes along the periodic structures may be bound on one side by an

effective low index of perforated alumina on the SiO_2 layer ($n_{Al2O3/SiO2}$~2) at the sample's bottom. On the other side of the sample where the graphene interfaces the porous alumina structure, the modes may be bound to the surface graphene guide by the low index of either air, or a combination of 200 nm polymer/air layer ($n_{air/polymer}$~1.15) (the polymer was a remnant of the graphene transfer process). In calculating the effective indices, we used the relative thicknesses of the various films. An approximation for the refractive index of graphene surface guide may make use of $\varepsilon(\omega)=\varepsilon_b+i\sigma_0/\omega d$: here $\varepsilon_b=5.8\varepsilon_0$ as the effective dielectric constant for graphene with a background material [32] and d=3.38 Angstroms for the effective graphene thickness and σ_0 is the graphene conductivity.

Electromagnetic radiation may be efficiently coupled with a surface mode when the wavevector of either the incident, or scattered (or both) waves are at resonance with the wavevector of the perforated substrate [28]. Since the array pitch is much smaller than the free-space wavelength, a surface mode may become a standing wave, as well. The positions of the QDs are in-phase with the standing electromagnetic surface modes, resulting in enhanced luminescence (Fig. 2).

The tilt angle θ that produces maximum coupling between the surface and radiation modes may be computed similarly to [33] as,

$$sin(\theta)=\frac{\lambda_0}{a}\sqrt{(\frac{4}{3})(q_1^2-q_1q_2+q_2^2)}-n_{eff} \quad (1)$$

Here, λ_0, is the incident or emitted wavelength, a, is the pitch for the holes array (a~90 nm), q_1 and q_2 are sub-integers (e.g., 1/3) representing the ratio between the array pitch and the propagating wavelength. Eq. (1) <u>*cannot be fulfilled*</u> for the pump wavelength of 488 nm and n_{eff}~2.4 for graphene guide in the range of tilt angles of $-8^o<\theta<8^o$. Therefore, the fluorescence

peaks in Fig. 2 ought to be attributed to the resonances at only *emission* wavelengths. Upon tilting the sample, there are two symmetric peaks in the fluorescence emission as per (1) at ca $\pm 2^{o}$.

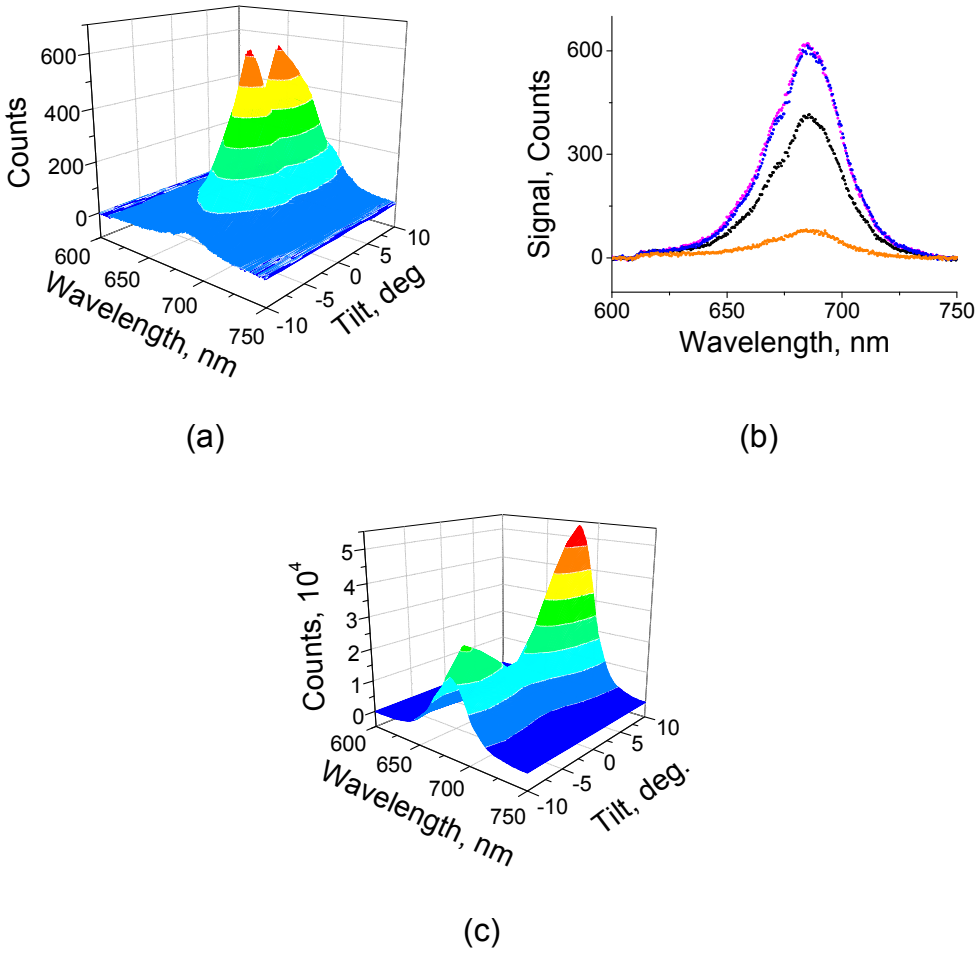

Fig. 2. (a) Fluorescence of QD690 embedded in graphene covered, AAO hole-array with a pitch of ca 90 nm. (b) A few curves at some specific tilt angles – no meaningful change in the linewidths as a function of tilt angle has been noted. (c) Fluorescence of QD690 embedded in bare AAO.

For QDs embedded in a bare AAO the position of FL peaks has changed to ca $\pm 8^{o}$ (Fig. 2c). This is consistent with Eq. 1; in absence of graphene, the effective refractive index has reduced, and the angle that satisfies Eq. 1 becomes larger.

IV. Results and Discussions:

The successful transfer of graphene to the QD loaded AAO hole-array was confirmed by measuring the Raman spectrum of the graphene before (not shown) and after transfer (Fig. 3). The spectrum was recorded at normal incidence. The relatively small 2D line could be attributed in part to the diminishing quantum efficiency of the Si- based CCD array. In general, the lines have been somewhat blue shifted [34] and could point to the effect of the hole-array on the graphene.

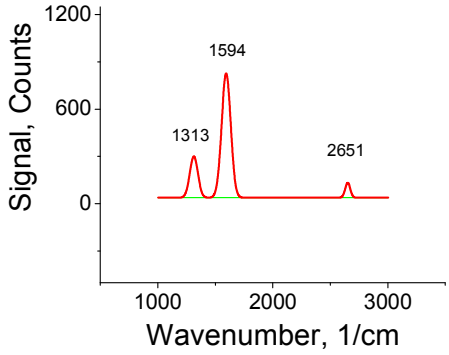

Fig. 3. Raman spectrum of graphene, interfaced with QDs. Data were taken with 11.5 mW 785 nm laser and an x50 LF objective. The small 2D peak is attributed to relatively large defect line at 1313 1/cm (due to contact with the QDs) and the low detector efficiency at that long wavelength (2700 1/cm translates to ~ 950 nm Stokes line).

The photoluminescence lifetime measurements were first conducted at normal incidence. The data have been fitted with three time-constants, which fell into three categories: τ_1<1 ns; τ_2~1 ns and τ_3~10 ns. In order to ensure the quality of the fit, the adjusted, or standard R^2 value has to be near 1 and the residuals have to be symmetrical. The very short life time (of the order of 200 ps) is similar to laser pulse duration and hence could be identified as system response or a stimulated effect. The very long time constant (of the order of 10 nsec) is typical of QDs albeit it is a bit

shorter compared to the literature [35] and our own data on glass. Its amplitude was typically half of the medium lifetime constant (of the order of 1 nsec). We attribute the latter to coupling of the radiation mode to the structured substrate (see below on the local energy density and its impact on the radiation lifetime). These lifetime constants correspond to transition rates, b, c, and d respectively (Fig. 4).

As noted in [36, 37], the local density of states may be modified by the immediate environment at the chromophore. Thus, our concept of quenching may well be determined by unknown molecular concentration, layer conductivity and the properties of the surface mode. Two examples are shown below: (a) a large transition rates (Fig. 4b) which were associated with unusual large luminesce; (b) ‘quenched’ luminescence (Fig. 5a, and Fig. 4) which was associated with smaller transition rates. The metal films were not perfect. 'Quenched' signals were typically obtained for QDs on a smooth metal environment. 'Enhanced' signals were typically obtained from relatively rough metal surfaces. The enhanced signals cannot be attributed to QDs situated at distances larger than the Förster length, because as the chromophores are placed away from the quenching layer, their related lifetimes should become longer (and not shorter, as observed here) when compared to their quenched signal counterparts [38]. Thus, these two cases represent uncertainties in the local QDs environment. QDs interfaced with conductive surfaces such as graphene and metal, do exhibit overall shorter emission lifetimes when compared to their non-interfaced counterpart.

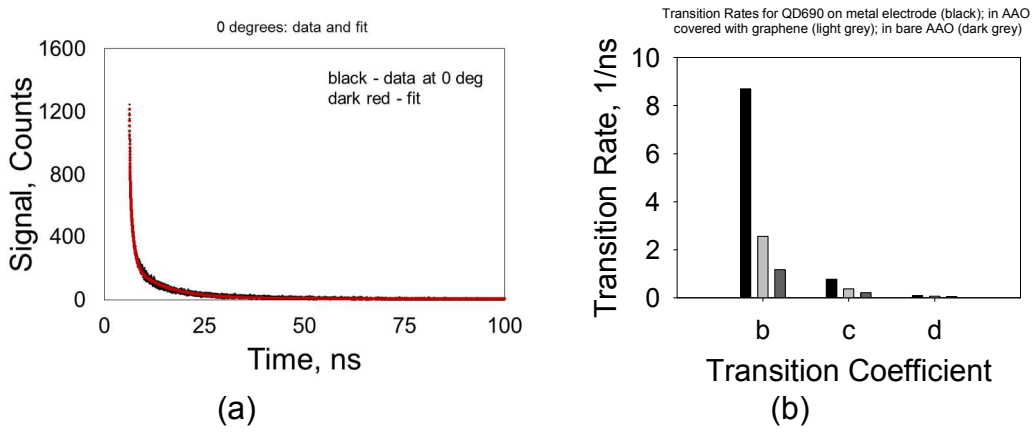

	on electrode	in AAO/graphene	in bare AAO
b	8.7±1.4	2.56±0.07	1.18±0.04
c	0.78±0.04	0.38±0.012	0.22±0.007
d	0.10±0.001	0.07±0.001	0.06±0.001

Fig. 4. (a) A typical temporal data and its fit at normal incidence (tilt angle, 0^{o}). (b) Various transition rates for QDs: on aluminum electrode (black) in AAO hole-array covered with graphene (light grey) and in bare AAO hole-array. The longest lifetime was measured for QD embedded in bare AAO where the shortest one was obtained for QD on the aluminum electrode. The table provides with the transition values in 1/ns. The transition values for QDs on the metal are associated with the larger luminescence signal of Fig. 5b. The values for the 'quenched' case (Fig. 5a) are respectively, b=2.58/ns; c=0.37/ns and d=0.07/ns; they are comparable to the graphene values but larger than the values for QDs embedded in bare AAO.

Complementary experiments were conducted on the line broadening of the fluorescence emission (Fig. 5). The spectrum was fitted with two Gaussian peaks whose position and width are provided by the accompanying table. Within the measurement error, no substantial change in the emission linewidth was noted as a function of tilt angle (Fig. 2b). However, as will be seen below, there is a marked change in the related emission lifetimes. One may observe two cases measured for two spots on the aluminum electrode: one shown in Fig. 5a is a 'quenched' case, whereas, the one shown in Fig. 5b is an 'enhanced' case. The fluorescence intensity was quenched as expected when the QDs were interfaced with the graphene or the aluminum electrode. This was accompanied by a clear linewidth broadening but its relative emission rates

are smaller than the 'enhanced' case. We point out that the linewidth of the QDs is masked by an inhomogeneous broadening, attributed to size dispersion.

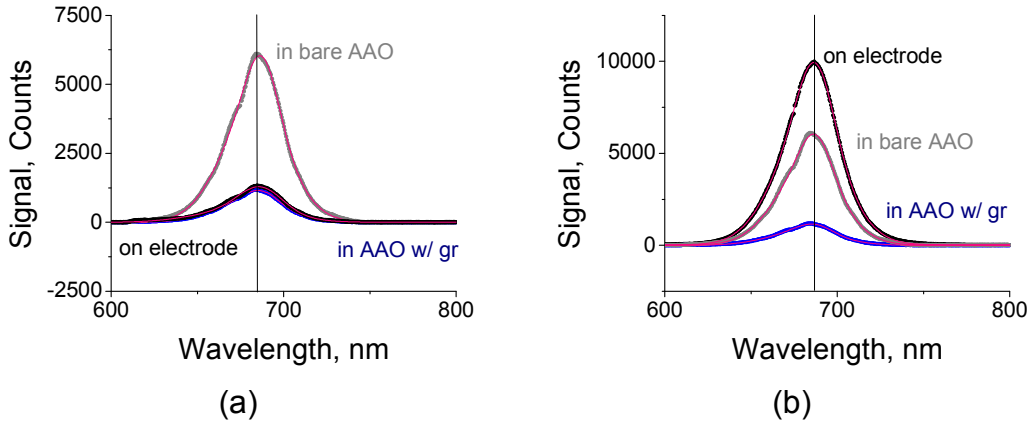

Table (a)

linewidth (nm)		on Al electrode	peak (nm)		in AAO/graphene	peak (nm)		in bare AAO	peak (nm)	
w1		50.1±0.51	675.36		39.63±0.20	680.26		37.98±0.17	682.6	
w2		25.07±0.25	686.72		19.85±0.27	686.98		18.47±0.22	687.75	

Table (b)

linewidth (nm)		on Al electrode	peak (nm)		in AAO/graphene	peak (nm)		in bare AAO	peak (nm)	
w1		39.99±0.10	683.17		39.63±0.20	680.26		37.98±0.17	682.6	
w2		20.58±0.10	687.62		19.85±0.27	686.98		18.47±0.22	687.75	

Fig. 5. (a) Linewidth of luminescence by QDs on aluminum electrode, in AAO hole-array covered with graphene and in bare AAO hole-array. Quenching of the fluorescence by the graphene and metal is clearly seen. The linewidths for ODs on the aluminum electrode or AAO covered with graphene is wider than for QDs imbedded in bare AAO holes. The tables summarize the results. Molecular concentration might be an issue when dealing with luminescence quenching as shown in (b) QDs on a 'hot' metal spot exhibited a much larger emission than the other two cases; nevertheless, the lineswidths were respectively, ca 40 nm and 20.6 nm, still larger than the width of QD in bare AAO. The corresponding lifetime constants were shorter, as well (Fig. 4, table).

Most puzzling is the increase in the emission photon lifetime for QDs interfaced with graphene at tilt angles that seem to be associated with resonance coupling between the surface and the emission modes. In Fig. 6 we show the various rate coefficients as a function of tilt angle. One expects that when at resonance, the measured emission would exhibit a shorter lifetime due to an increase in the density of states of its surface modes [22]. Similar experiments with QDs in bare

AAO yielded much smaller luminescence changes (less than 3% in the transition coefficients compared with a larger than 10% change for luminescence of QDs interfaced with graphene coated AAO) and therefore deemed inconclusive. Nevertheless, coupling to the radiation modes is strong as observed in Fig. 2c.

Fermi's Golden rule relates the transition rate of the QDs to the final density of states at the emission frequency. In principle, the emission from a QD may be funneled through several radiation venues (waveguide modes, resonance modes, surface modes, etc.,) each of which has a different local, or global density-of-states (DOS). These venues are not necessarily coupled together and the impact of their density-of-states may not be simply summed up as was done in [32]; the photon has a finite probability to decay via each of these channel outlets. In the case of graphene surface guides, tilting of the sample resulted in capturing a subset of these venues, e.g., decay through a collective surface guiding mode, whose density of states is smaller than the one that was measured at off-resonance [39]. Specifically, the DOS for a two-dimensional propagating surface guide is linearly proportional to the radial frequency, ω, whereas the DOS for a three-dimensional free space radiation mode is proportional to the radial frequency squared, ω^2. Thus, in principle, at off-resonance conditions, the emission from a single QD emitter may couple to a larger density of states pool, and therefore exhibits a shorter lifetime. As stated before, inhomogeneous line broadening as a result of QD size dispersion may have obscured linewidth effects as a function of tilt. All of that means that graphene is better at sustaining surface propagating modes.

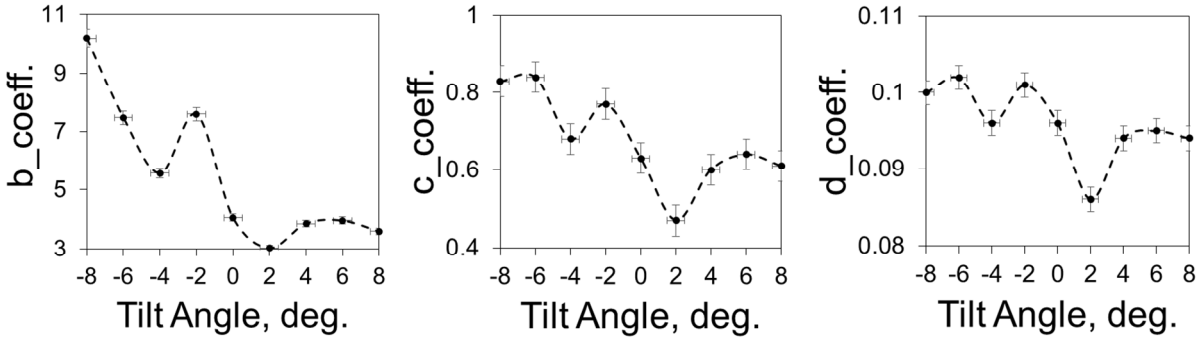

Fig. 6. The rate coefficients as a function of tilt angle. Close to resonance, these coefficients are at the minimum (suggesting longer photon lifetime) due to coupling to surface modes with lower density of states compared with their free-space counterparts. While there are variations due to local imperfections, the trend, as judged by the coefficients on either side of the minimum is nonetheless clear. The connecting dash curves are only guide to the eye.

In summary, we measured lifetime and linewidth for QDs on aluminum electrode, in AAO hole-array interfaced with graphene and compared it with QDs embedded in bare AAO hole-array. Indeed, QD interfaced with conductive films portrayed shorter lifetime and line-broadening but not necessarily fluorescence quenching.

Methods: 20 nm of SiO_2 of thermal oxide was deposited on a <100> p-type 1-10 Ohms.cm Si wafer. For the anodization, a 1-μm Al film was deposited on top of the SiO_2 layer; the Al was later anodized completely per previous recipe [29] – its final thickness was estimated as ~50 nm. Anodization of the Al resulted in a hole-array with a pitch of ca 90 nm and a typical hole-diameter of ca 20-30 nm. The hexagonal hole-array was polycrystalline with a typical domain size of ~10 μm. The CdSe/ZnS QDs with peak luminescence of ca 690 nm were suspended in toluene and drop-cast into the anodized porous substrate. The QDs were coated with octadecylamine to prevent agglomeration while in suspension. That ligand also prevented agglomeration within the pore and added thickness to the QD. We washed the sample and mechanically wipe it off with a wet lens tissue prior to coating the sample with graphene. That

procedure resulted in a very few QDs within the substrate pores (25 QDs/μm^2) and ascertained a single QD per pore. This procedure was found adequate for relatively large pores as well (<50 nm).

The graphene was produced by chemical vapor deposition (CVD) on copper foil and was transferred onto the QD embedded substrate by use of 200 nm poly(methyl methacrylate), PMMA film [40]. In some cases we retained the PMMA film as a protective upper coating. The presence of the PMMA did not affect the lifetime nor the spectral line widths.

Lifetime and spectral line width data were obtained using a microscope system (Olympus IX71) coupled to both a spectrometer with a CCD detector array and to a single photon avalanche photodiode (SPAD). The sample was excited with 488 nm pulses (19 μW, 5 MHz, 200 ps) from a supercontinuum laser (Fianium WhiteLase SC-390). The excitation wavelength was selected using an acousto-optic tunable filter (AOTF) along with a bandpass filter. A 5x objective (Olympus NeoSPlan, 0.13 NA) was used to both focus the excitation and collect the emission. A dichroic filter (Semrock FF506-Di03) was used to separate the excitation and emission wavelengths. For spectral measurements, the collected emission was directed to the entrance slit of a 300 mm focal length spectrometer (Acton, SP2300) equipped with a 150 l/mm diffraction grating and a 1320 x 100 channel CCD (Princeton Instruments, PIXIS 100BR). Time-resolved data was collected using the time-correlated single photon counting technique (TCSPC). For the TCSPC measurements, the collected emission from the sample was sent to a SPAD (MPD SPD) after passing through a long pass filter (Chroma, HQ520LP). The pulses from the SPAD were

recorded using a computer controlled TCSPC system (Picoquant, PicoHarp300). For the angle-resolved measurements, the sample was tilted with respect to the p-polarized laser (Fig. 1c).

Tilting of the sample was made by modifying the optical microscope to include a rotational stage instead of the tradition microscope platform. The spot position of the focused 488 nm pump beam was monitored by a separate CCD camera to help minimizing spot wobbling. Due to the relatively large pump spot, re-focusing was found un-necessary for angles smaller than 10 degrees; however, this may be of concern for tightly focused beams.

Acknowledgement: This work was performed, in part, at the Center for Nanoscale Materials, a U.S. Department of Energy Office of Science User Facility, and supported by the U.S. Department of Energy, Office of Science, under Contract No. DE-AC02-06CH11357.

References

1. Persson, B. N. J.; Lang, N. D., Electron-Hole-Pair Quenching of Excited-States near a Metal. Physical Review B 1982, **26**, 5409.
2. Barnes, W. L., Fluorescence near interfaces: the role of photonic mode density. Journal of Modern Optics 1998, **45**, 661.
3. P. R. Wallace, The Band Theory of Graphite, Phys. Rev., 1947, **71**, 622.
4. K.S. Novoselov, A.K. Geim, S.V. Morozov, D. Jiang, Y. Zhang, S.V. Dubonos, I.V. Grigorieva and A.A. Firsov, Electric Field Effect in Atomically Thin Carbon Films, | Science, 2004, **306**, 666-669.
5. A. C. Ferrari, J. C. Meyer, V. Scardaci, M. Lazzeri, F. Mauri, S. Piscance, D. Jiang, K. S. Novoselov, S. Roth and A. K. Geim, Raman Spectrum of Graphene and Graphene Layers, *Phys*. Rev. Lett., 2006, **97**, 187401.
6. Alexander V. Klekachev, Amirhasan Nourbakhsh, Inge Asselberghs, Andre L. Stesmans, Marc M. Heyns, and Stefan De Gendt, Electron accumulation in graphene by interaction with optically excited quantum dots, Physica E 2011, **43**, 1046–1049.
7. Haifeng Dong, Wenchao Gao, Feng Yan, Hanxu Ji, and Huangxian Ju, Fluorescence Resonance Energy Transfer between Quantum Dots and Graphene Oxide for Sensing Biomolecules, Anal. Chem., 2010, **82**, 5511–5517.
8. Weiyi Lin, Bo Tian, Pingping Zhuang, Jun Yin, Cankun Zhang, Qiongyu Li, Tien-mo Shih, and Weiwei Cai, Graphene-Based Fluorescence-Quenching-Related Fermi Level Elevation and Electron-Concentration Surge, Nano Letts, 2016, **16**, 5737−5741. DOI: 10.1021/acs.nanolett.6b02430

9. Konstantatos G, Badioli M, Gaudreau L, Osmond J, Bernechea M, Garcia de Arquer FP, Gatti F, Koppens FH. “Hybrid graphene-quantum dot phototransistors with ultrahigh gain”, Nat Nanotechnol. 2012, **7**, 363-8. doi: 10.1038/nnano.2012.60

10. Mingyue Zhu, Qian Liu, Wei Chen, Yuanyuan Yin, Lan Ge, Henan Li, and Kun Wang, Boosting the Visible-Light Photoactivity of BiOCl/BiVO4/N-GQD Ternary Heterojunctions Based on Internal Z-Scheme Charge Transfer of N-GQDs: Simultaneous Band Gap Narrowing and Carrier Lifetime Prolonging, ACS Appl. Mater. Interfaces, 2017, **9**, 38832–38841. DOI: 10.1021/acsami.7b14412.

11. Yanyan Zhu, Xin Meng, Huijuan Cui, Suping Jia, Jianhui Dong, Jianfeng Zheng, Jianghong Zhao, Zhijian Wang, Li Li, Li Zhang, and Zhenping Zhu, “Graphene Frameworks Promoted Electron Transport in Quantum Dot-Sensitized Solar Cells”, ACS Appl. Mater. Interfaces, 2014, **6**, 13833–13840. DOI: 10.1021/am503258x

12. Jing Chen, Feng Xu, Jun Wu, Khan Qasim, Yidan Zhou, Wei Lei, Li-Tao Suna and Yan Zhang, Flexible photovoltaic cells based on a graphene–CdSe quantum dot nanocomposite, Nanoscale, 2012, **4**, 441.

13. Y. L. Chen, Y. J. Ma, D. D. Chen, W. Q. Wang, K. Ding, Q. Wu, Y. L. Fan, X. J. Yang, Z. Y. Zhong, F. Xu, and Z., M. Jiang, Effect of graphene on photoluminescence properties of graphene/GeSi quantum dot hybrid structures, Appl. Phys. Lett. 2014, 105, 021104. doi: 10.1063/1.4889890

14. Omer Salihoglu, Nurbek Kakenov, Osman Balci, Sinan Balci and Coskun Kocabas, Graphene as a Reversible and Spectrally Selective Fluorescence Quencher, Scientific Reports, 2016, **6**, 33911. DOI: 10.1038/srep33911

15. Zheyuan Chen, Stéphane Berciaud, Colin Nuckolls, Tony F. Heinz and Louis E. Brus, Graphene channels interfaced with an array of individual quantum dots, arxiv.org/ftp/arxiv/papers/1003/1003.3027.pdf

16. Archana Raja Andrés Montoya−Castillo, Johanna Zultak, Xiao-Xiao Zhang, Ziliang Ye, Cyrielle Roquelet, Daniel A. Chenet, Arend M. van der Zande, Pinshane Huang, Steffen Jockusch, James Hone, David R. Reichman, Louis E. Brus, and Tony F. Heinz, Energy Transfer from Quantum Dots to Graphene and MoS2: The Role of Absorption and Screening in Two-Dimensional Materials, Nano Lett. 2016, **16**, 2328−2333, DOI: 10.1021/acs.nanolett.5b05012.

17. Benoît Rogez, Heejun Yang, Eric Le Moal, Sandrine Lévêque-Fort, Elizabeth Boer-Duchemin, Fei Yao, Young-Hee Lee, Yang Zhang, K. David Wegner, Niko Hildebrandt, Andrew Mayne, and Gérald Dujardin, Fluorescence Lifetime and Blinking of Individual Semiconductor Nanocrystals on Graphene, J. Phys. Chem. C 2014, **118**, 18445−18452. dx.doi.org/10.1021/jp5061446

18. Li R, Schneider LM, Heimbrodt W, Wu H, Koch M, Rahimi-Iman A, Gate Tuning of Förster Resonance Energy Transfer in a Graphene - Quantum Dot FET Photo-Detector, Sci Rep. 2016, **6**, 28224. doi: 10.1038/srep28224.

19. A. H. Castro Neto, F. Guinea, N. M. R. Peres, K. S. Novoselov and A. K. Geim, The electronic properties of graphene, Rev. Mod. Phys. 2009, 81, 109-162.

20. M. M. Fogler, D. S. Novikov, and B. I. Shklovskii, Screening of a hypercritical charge in graphene, PRB, 2007, **76**, 233402.

21. Kenneth W-K. Shung, Dielectric function and plasmon structure of stage-1 intercalated graphite, PRB, 1986, **34**, 979-973.

22. E. M. Purcell, Spontaneous Emission Probabilities at Radio Frequencies, Phys. Rev. 1946, **69**, 681.

23. Manuela Lunz, A. Louise Bradley, Wei-Yu Chen, Valerie A. Gerard, Stephen J. Byrne, Yurii K. Gun'ko, Vladimir Lesnyak, and Nikolai Gaponik, Influence of quantum dot concentration on Förster resonant energy transfer in monodispersed nanocrystal quantum dot monolayers, PRB 2010, **81**, 205316. DOI:https://doi.org/10.1103/PhysRevB.81.205316

24. Manuela Lunz, A. Louise Bradley, Valerie A. Gerard, Stephen J. Byrne, Yurii K. Gun'ko, Vladimir Lesnyak, and Nikolai Gaponik, "Concentration dependence of Förster resonant energy transfer between donor and acceptor nanocrystal quantum dot layers: Effect of donor-donor interactions", Phys. Rev. B 2011, **83**, 115423. doi.org/10.1103/PhysRevB.83.115423

25. A. Banerjee, R. Li and H. Grebel, Surface Enhanced Raman with Graphenated Anodized Aluminum Oxide Substrates: the Effect of Sub-Wavelength Patterns", Nanotechnology, 2009, **20**, 295502.

26. A. Banerjee and H. Grebel, Depositing Graphene Films on Solid and Perforated. Substrates, Nanotechnology, 2008, **19**, 1-5, art. no.365303.

27. Ruiqiong Li, and Grebel Haim, Surface Enhanced Fluorescence (SEF): Polarization Characteristics, IEEE Sensors, 2010, 10, 465-468. doi: 10.1109/JSEN.2009.2038513.

28. R. Li, A. Banerjee and H. Grebel, The possibility for surface plasmons lasers, Optics Express, 2009, **17**, 1622-1627.

29. A. Banerjee, R. Li and H. Grebel, Surface plasmon lasers with quantum dots as gain media, Appl. Phys. Letts., 2005, **95**, 251106. doi:10.1063/1.3276273.

30. The linear absorption cross-section of the QD is $\sigma\sim(5x10^5)(D/2)^3$/cm as per C. A. Leatherdale, W.-K. Woo, F. V. Mikulec, and M. G. Bawendi, On the Absorption Cross Section of CdSe Nanocrystal Quantum Dots, J. Phys. Chem. B 2002, **106**, 7619-7622. Our dot diameter is D~10 nm [see 31]. If we assume that the absorption behaves as [1-*exp*[$-\sigma\cdot(N/V)\cdot D$]~ $\sigma\cdot(N/V)\cdot D$, with N the number of QD per volume V. The absorption is then A= $\sigma\cdot(N/V)$. Based on SEM, we estimated the concentration of dots as 25 QD/μm^2. Thus, the absorption of the QDs film is estimated as 0.016%.

31. W. William Yu, Lianhua Qu, Wenzhuo Guo, and Xiaogang Peng, Experimental Determination of the Extinction Coefficient of CdTe, CdSe, and CdS Nanocrystals, Chem. Mater. 2003, **15**, 2854-2860.

32. E. H. Hwang and S. Das Sarma, Dielectric function, screening, and plasmons in 2D graphene, http://arxiv.org/abs/cond-mat/0610561v3.

33. H. Grebel, Linear and nonlinear phenomena with resonating surface polariton waves and their applications, in Structured Surfaces as Optical Metamaterials, Alexei A. Maradudin. Editor, Cambridge, 2011

34. H. Paraskevaidis, T. Kuykendall, M. Melli, A. Weber-Bargioni, J. Schuck, A. Schartzberg, S. Dhuey, S. Cabrini and H. Grebel, Gain and Raman line-broadening with graphene coated diamond-shape nano-antennas, Nanoscale, 2015, **7**, 15321-31. DOI: 10.1039/C5NR03893F.

35. Adolfas K. Gaigalas, Paul DeRose, Lili Wang, and Yu-Zhong Zhang, Optical Properties of CdSe/ZnS Nanocrystals, Journal of Research of the National Institute of Standards and Technology, 2014, **119**. dx.doi.org/10.6028/jres.119.026.

36. Karl Joulain, Re´mi Carminati, Jean-Philippe Mulet, and Jean-Jacques Greffet, Definition and measurement of the local density of electromagnetic states close to an interface, Phys. Rev. B, 2003, **68**, 245405.

37. Per Lunnemann and A. Femius Koenderink, The local density of optical states of a metasurface, Scientific Reports, 2016, **6**, 20655. DOI: 10.1038/srep20655.

38. Sebastian Jander, Andreas Kornowski, and Horst Weller, Energy Transfer from CdSe/CdS Nanorods to Amorphous Carbon, Nano Letts., 2011, **11**, 5179–5183. dx.doi.org/10.1021/nl202370q

39. This point was raised by J. Grebel of U. Chicago.

40. Xuesong Li, Yanwu Zhu, Weiwei Cai, Mark Borysiak, Boyang Han, David Chen, Richard D. Piner, Luigi Colombo and Rodney S. Ruoff, Transfer of Large-Area Graphene Films for High-Performance Transparent Conductive Electrodes, Nano Letts, 2009, **9**, 4359-4363.